lncTIM3 promotes osteogenic differentiation of bone marrow mesenchymal stem cells via miR-214/Smad4 axis to relieve postmenopausal osteoporosis

Haitao Sun
Wuxi Huishan District People ' s Hospital
Lining Wang
Nanjing University of Traditional Chinese Medicine
muzhe li
Nanjing University of Traditional Chinese Medicine
Bin Xu
Wuxi Huishan District People ' s Hospital
Yong Ma
Nanjing University of Chinese Medicine
Yuanyuan Niu
Nanjing University of Chinese Medicine
Tianchi Zhang
Nanjing University of Chinese Medicine
Weiqing Qian
Nanjing University of Traditional Chinese Medicine
Xudong Chu (369341028@qq.com)
Wuxi Huishan District People ' s Hospital

Research Article

Keywords: postmenopausal osteoporosis, lncTIM3, bone marrow mesenchymal stem cells (BMSCs), osteogenic differentiation, Smad4

Posted Date: June 13th, 2023

DOI: https://doi.org/10.21203/rs.3.rs-3046391/v1

Abstract

Background

Promoting osteogenic differentiation of bone marrow mesenchymal stem cells (BMSCs) is the main therapeutic goal for postmenopausal osteoporosis (PMOP). Recently, several long non-coding RNAs (lncRNAs) have been reported to be involved in PMOP; however, the role of lncRNA tissue inhibitor of metalloproteinases 3 (lncTIM3) remains to be investigated.

Methods

The characteristics of BMSCs isolated from the PMOP rat model were verified by flow cytometry assay, alkaline phosphatase (ALP), alizarin red and Oil Red O staining assays. Micro-CT and HE staining assays were performed to examine histological changes of the vertebral trabeculae of the rats. RT-qPCR and western blotting assays were carried out to measure the RNA and protein expression levels. The subcellular location of lncTIM3 was analyzed by FISH assay. The targeting relationships were verified by luciferase reporter assay and RNA pull-down assay.

Results

The trabecular spacing was increased in the PMOP rats, while ALP activity and the expression levels of Runx2, Col1a1 and OCN were all markedly decreased. Among the RNA sequencing results of the clinical samples, lncTIM3 was the most downregulated differentially expressed lncRNA, also its level was significantly reduced in the OVX rats. Knockdown of lncTIM3 inhibited osteogenesis of BMSCs, whereas overexpression of lncTIM3 exhibited the reverse results. Subsequently, lncTIM3 was confirmed to be located in the cytoplasm of BMSC, implying its potential as a competing endogenous RNA for miRNAs. Finally, the negative targeting correlations of miR-214 between lncTIM3 and Smad4 were elucidated *in vitro*.

Conclusion

lncTIM3 attenuated PMOP via miR-214/Smad4. Possibly, these findings provided lncTIM3 as a therapeutic molecule for PMOP.

1 Introduction

Postmenopausal osteoporosis (PMOP) is a systemic and chronic bone disease caused by reduced estrogen in postmenopausal women due to ovarian function failure, and it is one type of primary osteoporosis [1]. PMOP may cause a series of bone remodeling disorders, such as bone microstructure degradation, bone density reduction, and bone fragility increment [2]. The fracture rate of PMOP patients

is three times higher than that of normal people [3]. Furthermore, fracture-caused bone deformation and other complications will greatly increase the disability rate of PMOP patients [3]. Studies have reported that the worldwide incidence of PMOP increases by 18% every 5 years [4]. On account of the high fracture and disability risks, PMOP severely impacts the life qualities of postmenopausal women. To date, the National Institutes of Health (NIH) has listed it as a global public health disease [5]. Hence, identification of novel therapeutic methods for PMOP has become an urgent clinical task.

The pathogenesis of PMOP is osteopenia, so promoting bone formation becomes a vital mechanism to postpone PMOP development. Bone formation mainly relies on intramembranous ossification and endochondral ossification, and both of which are initialed by differentiated mesenchymal stem cells [6]. Bone marrow-derived mesenchymal stem cells (BMSCs) are adult stem cells with self-renewal and multi-differentiation capabilities [7]. Under different inductions, BMSCs can differentiate into osteoblasts, adipocytes chondrocytes and neuroblasts [8]. Whether osteoblasts differentiate and mature from BMSCs is a prerequisite for bone formation [9]. Therefore, inducing the directional differentiation of BMSCs into bone tissues is significant for the repair of bone defects and the treatment of PMOP. Generally, Runx2, Type I Collagen (Col1a1) and osteocalcin (OCN) are used as indicators for osteogenic differentiation; alkaline phosphatase (ALP) activity is also positively correlated with the degree of osteogenic differentiation [10]. However, osteogenic differentiation is a complex network including regulation of multiple signaling pathways at transcriptional and post-transcriptional levels [11], the specific mechanism is still unclear.

91% of the gene sequences in the human genome are transcribed into non-coding RNAs (ncRNAs), among which long non-coding RNA (lncRNA) is a type of ncRNA that consists of more than 200 nucleotides [12]. lncRNAs extensively participate in biological processes, such as cell cycle, cell differentiation, transcription, translation and splicing [13]. Cell differentiation is an essential transcriptional output of the genome, and its dysregulation is related to numerous human diseases [14]. Specifically, lncRNAs achieve regulatory functions in cell differentiation through sponging miRNAs or competitively binding to mRNAs with miRNAs [15]. Currently, overwhelming studies have demonstrated that lncRNAs take part in osteoblast differentiation and maturation [16]. They can regulate BMSCs differentiation, expressions of osteogenic differentiation-related biomarkers (Runx2, OCN, Col1a1, ALP) and bone morphogenetic proteins [15]. Tissue inhibitor of metalloproteinases 3 (TIM3) belongs to TIMP family and is closely related to extracellular matrix [17]. However, the functions of lncTIM3 are poorly understood in PMOP. Herein, we intended to investigate the correlation between lncTIM3 and BMSCs differentiation, so that to open up a novel therapeutic target for PMOP.

2 Methods and materials

2.1 Clinical samples

Bone marrow samples from the PMOP patients (n = 3) and healthy individuals (n = 3) were collected from 2019.12 to 2021.12 in Third Affiliated Hospital of Nanjing University of Traditional Chinese Medicine

hospital. The PMOP samples were collected during marrow reaming, and the bone marrow discarded during the surgery of hip fracture female patients were obtained as control. Patients were diagnosed with PMOP according to the diagnostic criteria [18]. The inclusion criteria for the enrolled donors were: 1) menopause for 1 year or more; 2) patients with traumatic fractures aged from 55 to 70 years old; 3) underwent surgery within 4 days after fracture. Patients receiving hormonotherapy, drug therapy, with severe mental, metabolic diseases or organ failures were excluded from this study. This study was approved by the Ethics Committee of Third Affiliated Hospital of Nanjing University of Traditional Chinese Medicine Hospital (approval no. KY2017004) and strictly observed the Declaration of Helsinki. All samples were anonymous, and signed informed consents were obtained from each individual.

2.2 Animal model

All procedures were approved by the Animal Care and Use Committee of Third Affiliated Hospital of Nanjing University of Traditional Chinese Medicine Hospital. A total of fifty female Sprague Dawley rats (weight: 210 ± 8 g, age: seven weeks) were obtained from Shanghai Jake Biotech Co., Ltd. They were raised in pathogen free conditions with 12 h dark/light in separate cages, supplying with food and sterile water. After they acclimatized to the condition, the rats were divided into PMOP group (n = 15) and sham group (n = 15). Bilateral ovariectomy (OVX) was performed in PMOP group as previously described [19]. Briefly, the rats were first anesthetized with 30mg/kg pentobarbital sodium i.p. Ovaries were exposed then resected after tubal and vascular ligation under aseptic conditions. Rats in the sham group underwent the similar operation with OVX rats excepted for ovary resection. After operation, the rats were raised for 21 days and the levels of osteogenic differentiation related markers, including Runx2, Col1a1 and OCN were measured. At the end of the experiments, all rats were sacrificed by 150 mg/kg pentobarbital sodium i.p.

2.3 Micro computered tomography (CT)

The vertebral bone trabecula was visualized using the Skyscan 1273 3D X-ray microscopic imaging system (Bruker Daltonics). Regions of interest were defined from 0 image slice to 200 image slices, where the growth plate slice was defined as 0 image slice. The standardized region of femurs were scanned at 9-μm resolutions.

2.4 H&E staining

The L4 vertebra samples were sliced and fixed with 10% formaldehyde (F140859; Aladdin Biochemical Technology Co., Ltd.), dehydrated with ethyl alcohol, then embedded in paraffin, sliced into 5 μm thickness. The slides were stained with hematoxylin and eosin as previously described [20]. Five fields of the stained slide were randomly captured by an optical microscope (DM500; Leica Inc.).

2.5 Isolation, culture and treatment of BMSCs

0, 3, 7, 14 or 21 days after OVX, BMSCs were isolated from bilateral femurs and then cultured in DMEM with 10% FBS, 100 U/ml streptomycin and 100 U/ml penicillin (all obtained from Gibco) at 37°C under the presence of 5% CO_2. After cell confluence reached 80%, the cells were used for subculture. Passage 3 BMSCs were employed in the further experiments.

BMSCs in the logic growth phase were collected and transfected with short hairpin RNA of lncTIM3 (sh-lncTIM3), pcDNA3.1/lncTIM3, miR-214 inhibitor, miR-214 agomir, pcDNA3.1/Smad4 and their negative control (Beijing Ruibiotech Co., Ltd.) using Lipofectamine® 2000 reagent (Invitrogen) for 24 h according to different assays.

2.6 Flow cytometry assay

2×10^5 BMSCs at passage three were trypsinized. Then, 100 μl of PBS and 10 μl of the monoclonal antibodies, including CD73-PE (abx139794), CD90-PE (abx200917), CD95-FITC (abx139052), CD11-PE (abx200676), CD34 (abx200773) and CD45-PE (abx159410) were added to the cells to incubate for 20 min under darkness. FITC-labeled IgG antibody (abx140320; all from Abbexa) was used as the control group. After rinsed twice with PBS, surface antigens of the cells were analyzed using a FACS Calibur Flow Cytometer (BD Bioscience).

2.7 Induction of BMSCs differentiation

BMSCs were cultured in osteogenic induction medium (α-MEM containing 10%FBS, 10mM β-sodium glycerophosphate, 0.1μm hexadecadrol, 0.2mM vitamin C) or adipogenic induction medium (α-MEM containing 10%FBS, 0.01μm hexadecadrol, 0.5mM IBMX, 60μm indometacin, 2mM insulin) to induce osteoblast or lipoblast differentiation, respectively. During the induction period, the medium was renewed every 3 days.

2.8 Alizarin red, Oil red O and alkaline phosphatase (ALP) staining assays

7 days after osteogenic induction, BMSCs were stained with ALP (C3206; Beyotime Biotech Co., Ltd.) and alizarin red (G1452; Solarbio Technology Co., Ltd.) following the manufacturer's protocols, and ALP activities were quantified. 10 days after adipogenic induction, BMSCs were stained with Oil Red O (G1262; Solarbio). The stained cells were observed under optical microscope.

2.10 RNA sequencing

The total RNA was extracted using TRIzol® reagent and purified by DNase I (10607ES15; Shanghai Yeasen Biotech Co., Ltd.), respectively. After the total RNA was qualified, Epicentre Ribo-Zero™ Kit (ZhongBei LinGe Biotechnology Ltd.) was used to remove the rRNAs. Then the RNA was degraded into 200–500 bp fragments with fragmentation buffer (Agilent Technologies, Inc.). The chain specific cDNA library was obtained by PCR amplification. The Illumina HiSeq™ 2500 was used to perform RNA sequencing.

2.11 Real-time quantitative polymerase chain reaction (RT-qPCR)

The BMSCs and homogenized vertebral tissues were mixed with TRIzol® reagent (Invitrogen) to extract total RNA. Reverse transcription and amplification were performed using EzOmics™ One-Step qPCR Kit

(BK2100; Biomics Biotech) on GeneAmp PCR System 9700 (Applied Biosystems). All primers were designed and synthesized by Abace Biotech Co., Ltd., GAPDH and U6 were used as internal reference for mRNAs and miRNA, respectively. Fold changes of the RNAs were assessed using $2^{-\Delta\Delta Ct}$ method. The sequences of the primers used were as followed: Runx2 forward 5′-CCAGAATGATGGTGTTGACG-3′ and reverse 5′-GGTTGCAAGATCATGACTAGGG-3′; Col1a1 forward 5′-GAGGGCCAAGACGAAGACATC-3′ and reverse 5′-CAGATCACGTCATCGCACAAC-3′; OCN forward 5′-AGCAAAGGTGCAGCC TTTGT-3′ and reverse 5′-GCGCCTGGGTCTCTTCACT-3′; lncTIM3 forward 5′- CCAGCAGAGACACAGACACT – 3′ and reverse 5′-TTGCTCCAGAGTCCCGTAAG-3′; miR-214 forward

5′-CAGGACAGCAGGCACAGACA-3′ and reverse 5′-TCAACTGGTGTCGTGGAGTC-3′; Smad4 forward 5′-GGGCAGCGTAGCATATAAGA-3′ and reverse 5′-GACCCAAACGTCACCTTCAG-3′; GAPDH forward 5′-ACCCACTCCTCCACCTTTGAC-3′ and reverse 5′-TGTTGCTGTAGCCAAATTCGTT-3′; U6 forward 5′-GCTTCGGCAGCACATATACTAAAAT-3′ and reverse 5′-CGCTTCACGAATTTGCGTGTCAT-3′.

2.12 Western blotting assay

Proteins of BMSCs and vertebral tissues were extracted using RIPA lysis buffer (R0010; Solarbio). The proteins were quantified with the BCA Protein Assay Kit (abs9232; Absin Biotech Co., Ltd.). 40 μg of the protein was separated on 10% SDS-PAGE maintained for 1.5 h at 120 V. Afterwards, the separated proteins were transferred onto PVDF membranes (V273606; Bio-rad Laboratories) for 2 h at 200 mA. BSA was used to block the proteins for 1 h. Then the membranes were incubated with following primary antibodies: anti-Runx2 (1:1000; 70R-49481), anti-Col1a1 (1:800; 70R-14951), anti-OCN (1:400; 10R-10328), anti-Smad4 (1:1000; 70R-31865) and anti-GAPDH (1:1000; 70R-33170) at 4˚C overnight. Next day, the membranes were incubated with a mouse anti human IgG secondary antibody (1:4000; 43-1003; all from Fitzgerald) at room temperature for 2 h. Finally, the protein expressions were analyzed using the Super ECL Detection Reagent (36208ES60; Yeasen Biotechnology Co., Ltd.). GAPDH was used as an internal reference.

2.13 Fluorescence in situ hybridization (FISH) assay

lncTIM3 subcellular localization in BMSC was analyzed by the Ribo™ lncRNA FISH Probe Mix (Red) (C10920; Guangzhou Ribobio Co., Ltd.) according to the manufacturer's protocol. Briefly, the cells were inoculated into a 48-well plate at the density of 1×10^4 and the medium was discarded. The cells were rinsed with PBS twice then fixed with 4% paraformaldehyde for 15 min. Next, the cells were hybridized with the Cyanine dye 5 (Cy5)-labeled lncTIM3 probes at 37°C overnight. The next day, the probe mixture was discarded, and the BMSCs were counterstained with DAPI. The cells were observed and captured under fluorescence microscope.

2.14 Luciferase reporter assay

The wild (WT) and mutant (MUT) types 3′-UTR regions of lncTIM3 and Smad4 luciferase reporter vectors were synthesized by Shanghai Hanheng Biotech Co., Ltd. They were transfected into BMSCs and incubated for 24 h, respectively. Whereafter, cells were lysed to detect the luciferase activities using the

Highly Stable Luciferase Reagent Kit (KA3728; Abnova Biotech Co., Ltd.) after 48 h co-transfection with the luciferase reporter vectors and miR-214 mimics. The luciferase activity was normalized to *Renilla* luciferase activity.

2.15 RNA pull-down assay

MagCapture™ RNA Pull Down Assay Kit (297-77501; FUJIFILM Wako Co., Ltd.) was used to conducted RNA pull-down assay. The biotinylated lncTIM3 probe and its control probe were synthesized by Abiocenter Co., Ltd. Briefly, the probe was incubated with 50 μl streptavidin-coated magnetic beads at 4˚C for 2 h. At the end of incubation, BMSCs were lysed to release the total RNA, and the beads were subsequently eluted. After separation, RT-qPCR and western blotting assays were used to quantify the relative expressions of miR-214 and Ago2 as described above.

2.16 Statistics

Each experiment was performed for triplication. Data were analyzed by GraphPad Prism (version 9.1.1.225, GraphPad Software Inc.). The data were presented as mean ± SD. Student t-test was performed for the two-group comparison, and analysis of variance (ANOVA) was used for the comparison among multiple groups followed by Duncan's post-hoc test. Pearson correlation analysis was carried out to assess the correlation. $P < 0.05$ was deemed as significant difference.

3 Results

3.1 Characteristics of BMSCs

BMSCs isolated from bilateral femurs of the mice were applied to flow cytometry assay to detect positive rates of the surface markers at passage three. As shown in Fig. 1A, BMSCs were positive for CD73, CD90 and CD95, while negative for CD11, CD34 and CD45, which was consistent with the characteristics of MSCs [21]. Under optical microscope, cells were observed as spiral shapes when cell confluence reached 90% (Fig. 1B). Furthermore, alizarin red (Fig. 1C) and ALP (Fig. 1D) staining images exhibited that BMSCs had potential in osteogenic differentiation; meanwhile, Oil red O (Fig. 1E) image demonstrated adipogenic differentiation ability of BMSCs.

3.2 Osteogenic rate was decreased in OVX rats

After the PMOP rat model was established, the pathological changes in vertebra of the OVX rats were examined compared to the sham rats. Significant increments in trabecular spacing were observed in micro-CT (Fig. 2A) and HE (Fig. 2B) staining images in the OVX rats, indicating that trabecular bone loss was accelerated. In addition, ALP activity was notably decreased in the OVX rats, which further provided evidence for the pathological images (Fig. 2C). In addition, mRNA expressions of the osteogenesis-related genes, including Runx2, Col1a1 and OCN (Fig. 2D-F) were detected at day 0, 3, 7, 14, 21 after operation to estimate the osteogenic differentiation ability of the rats and they were all markedly reduced in the OVX rats 21 days after modeling, indicating OVX impaired osteogenic differentiation potential in rats.

3.3 lncTIM3 promoted osteogenic differentiation of BMSCs

Ulteriorly, the underlying mechanism of decreased osteogenic rate in PMOP was investigated. RNA sequencing analyzed the differentially expressed (DE) lncRNAs in the clinical samples (Fig. 3A), among which lncTIM3 was the most downregulated DE lncRNA (Fig. 3B). Additionally, lncTIM3 level in the OVX rats were significantly decreased 7 days after modeling (Fig. 3C). Thus, we selected lncTIM3 for the following research. Sh-lncTIM3 decreased the expression level of lncTIM3 in BMSCs isolated from the sham rats, while pcDNA3.1/lncTIM3 exhibited the reverse results in BMSCs isolated from the OVX rats (Fig. 3D). ALP positive cells was reduced in sh-lncTIM3 transfected BMSCs, but enhanced in lncTIM3 overexpression BMSCs (Fig. 3E). Similarly, the mRNA (Fig. 3F) and protein (Fig. 3G and H) expression levels of Runx2, Col1a1 and OCN were decreased by sh-lncTIM3, while increased by pcDNA3.1/lncTIM3.

3.4 lncTIM3 served as a molecular sponge for miR-214 in BMSCs

Considering lncTIM3 could facilitate osteogenesis in the OVX rats, the specific regulatory mechanism related to lncTIM3 was further explored. As displayed in Fig. 4A, lncTIM3 was mainly located in the cytoplasm of BMSCs, suggesting that lncTIM3 might exert its functions as a competitive endogenous RNA (ceRNA). Recently, a meta-analysis indicated that miR-214 was the most significantly upregulated miRNA in BMSCs of OVX mouse model [22]. On this basis, we utilized RNAhybrid function of the online bioinformatic tool (https://bibiserv.cebitec.uni-bielefeld.de/rnahybrid?id=rnahybrid_view_submission) to for sequences of lncTIM3 and miR-214, and it turned out that they had binding sequences. The 3'-UTR sequences of WT and MUT lncTIM3 were cloned into the luciferase reporter vectors (Fig. 4B, up). In the WT lncTIM3 group, miR-214 mimic markedly weakened the luciferase activity; reversely, miR-214 inhibitor enhanced the luciferase activity. However, no significant change was observed in the MUT lncTIM3 group (Fig. 4B, down). Furthermore, biotinylated lncTIM3 prominently enriched Ago2 (Fig. 4C) and miR-214 (Fig. 4D) in BMSCs. miR-214 was dramatically upregulated in the PMOP patients (Fig. 4E) as well in the OVX rats (Fig. 4F), which was in line with the results above. Knockdown of lncTIM3 elevated the level of miR-214, while lncTIM3 overexpression exhibited the reverse result in BMSCs (Fig. 4G). Finally, Pearson correlation analysis revealed that the expression levels of lncTIM3 and miR-214 were negatively correlated (Fig. 4H).

3.5 miR-214 inhibitor abrogated the effects of sh-lncTIM3

The functional experiments were subsequently performed to verify the correlation between lncTIM3 and miR-214. sh-lncTIM3 reduced the APL-positive BMSCs, while miR-214 inhibitor reversed the reduction (Fig. 5A). The similar trends were also observed in the mRNA (Fig. 5B) and protein (Fig. 5C) expression levels of Runx2, Col1a1 and OCN.

3.6 Smad4 was the target gene of miR-214

According to Fig. S1, differentially expressed genes were sequenced in the clinical samples and we found that the PMOP DEGs were enriched in the osteogenic differentiation signaling pathway. Subsequently, we screened for the target genes of miR-214 using TargetScan (http://www.targetscan.org/vert_71/) and miRWalk (http://mirwalk.umm.uni-heidelberg.de/). We compared the predicting results and the sequencing results of the clinical samples, and Smad4 was the intersection of the two results. As known, Smad4 is a signal transduction molecule of BMP2, which is an important signal pathway regulating osteogenic differentiation, and it is a marker for osteogenic differentiation [23]. Protein expression level of Smad4 was significantly decreased when lncTIM3 was inhibited in the BMSCs from the rat model, while increased when lncTIM3 was overexpressed (Fig. 6A and B). However, no statistical change was observed in mRNA expression level of Smad4 (Fig. 6C), implying that it might receive post-transcriptional regulation as a target gene of miR-214. The luciferase reporter vectors of WT and MUT Smad4 were constructed (Fig. 6D). The luciferase activity of WT Smad4 was markedly decreased by miR-214 mimic, while enhanced by miR-214 inhibitor. In addition, no significant change was observed in the MUT Smad4 group (Fig. 6E). As expected, protein expressions of Smad4 were inhibited in 3 groups of OVX animal model and PMOP clinical samples (Fig. 6F). Positive correlation was assessed between the expression of lncTIM3 and Smad4 (Fig. 6G).

3.7 Rescue of Smad4 reversed the effects of miR-214

Finally, Smad4 was rescued in BMSCs and cellular epigenetic changes were assessed to verify the functional correlation between miR-214 and Smad4. The mRNA expression of lncTIM3 and protein expression of Smad4 were enhanced, while miR-214 was decreased when lncTIM3 was overexpressed in BMSCs; however, miR-214-agomir reversed the results. Besides, overexpression of Smad4 restored the levels of Smad4 in miR-214 overexpression BMSCs (Fig. 7A and B). Similar results to Smad4 were observed in ALP activity (Fig. 7D), mRNA (Fig. 7C) and protein (Fig. 7E and F) expressions of Runx2, Col1a1 and OCN.

4 Discussion

PMOP, which is triggered by estrogen reduction, induces osteopenia even fracture in elder women [3]. Consequently, the present study mainly aim at accelerating osteogenic differentiation of BMSCs to ameliorate PMOP. lncRNAs are widely reported to participate in the progression of PMOP [24]; nevertheless, the functional interaction between lncRNAs and BMSCs are rarely investigated. Herein, we found that lncTIM3 was downregulated in PMOP patients and OVX rats. Inversely, overexpression of lncTIM3 had promotive effects on osteogenic differentiation of BMSCs, and the effects were achieved through miR-214/Smad4 axis. These data proposed a novel aspect for PMOP treatment.

According to the previous researches, lncRNAs exert efficient therapeutic roles in PMOP. For example, lncMEG3 expression level was markedly lifted in BMSCs of the PMOP patients, while decreased during the differentiation of BMSCs to osteoblasts [25]. Li et al. demonstrated that lncCRNDE was upregulated in osteoclasts from the PMOP patients (OP). Meanwhile, knockdown of CRNDE in OP decreased cell

viability, increased apoptosis rate and arrested cell cycle in G0/G1 phase [24]. Moreover, lncDGCR5 was inhibited in hMSCs of the PMOP patients, but upregulation of lncDGCR5 facilitated osteogenic differentiation of hMSCs [26]. As for the effects on BMSCs, lncGAS5 expression was decreased in the BMSCs from OVX mice; whereas, excess amount of GAS5 promoted BMSC osteogenic differentiation [27]. Depletion of lnc_000052 accelerated BMSC cell growth, metastasis, osteogenic differentiation through PI3K/Akt signaling pathway [28]. In the current study, we found that lncTIM3 was significantly downregulated in the PMOP samples. Besides, overexpression of lncTIM3 enhanced, whereas inhibition of lncTIM3 slowed osteogenesis of BMSCs. As far as we know, these findings first elucidated the pro-osteogenesis function of lncTIM3, which filled the knowledge gap in the field of PMOP.

In PMOP, the regulatory functions of numerous miRNAs have been identified. For example, downregulation miR-155 [29] and miR-182 [30] could promote the osteogenic differentiation of BMSCs. lncRNAs generally serve as ceRNAs that competing for miRNAs to mediate the epigenetic regulation [28]. In the present report, we found that lncTIM3 was located in the cytoplasm of BMSCs, implying lncTIM3 might target for miRNAs to exert its role in PMOP treatment, and miR-214 was ulteriorly verified to be the target of lncTIM3. miR-214 is mostly studied in oncology [31–33]. Besides, miR-214 was previously demonstrated to regulate osteogenic differentiation potential of BMSCs. Yang et al. found that miR-214 was upregulated in MSCs of PMOP mice; whereas, inhibition of miR-214 promoted the osteogenic differentiation of MSCs, and this promotion was achieved by restoring FGFR1 protein expression [34]. Plasma miR-214 level was elevated in catagmatic patients. However, inhibition of miR-214 increased the expressions of COL1A1 and COL-X, but decreased COL-II expression [35]. In our study, inhibition of miR-214 restored osteogenic differentiation abilities of BMSCs suppressed by lncTIM3 knockdown as evident by increased Runx2, Col1a1, OCN and ALP levels, which was in line with the previous researches.

Smad4 has been widely discussed in osteogenesis because it is the pivotal molecule linking bone morphogenetic protein (BMP) and TGF-β signals. In 2013, it was found that knockdown of Smad4 in osteoblasts inhibited the formation of bone matrix and exacerbated dysosteogenesis in mice. Moreover, the mice suffered from severe growth arrest and malocclusion, causing difficulties in survival for 8 weeks [36]. Smad4 was decreased in TNF-α-induced BMSCs, while overexpression of Smad4 promoted osteogenesis [37]. And in many cases, Smad4 was targeted by miRNAs to trigger osteoporosis, such as miR-137 [38], miR-1323 [39] and miR-664-3p [40]. In the present study, we confirmed that Smad4 was the target gene of miR-214, and overexpression of Smad4 abrogated the decreased osteogenic rate induced by miR-214 in BMSCs, which was in accordant with the previous studies.

In conclusion, lncTIM3 was downregulated in PMOP, and overexpression of lncTIM3 accelerated osteogenesis of BMSCs via miR-214/Smad4 axis. These findings revealed the potent therapeutic effects of lncTIM3 in PMOP, developing a novel aspect for PMOP treatment.

Declarations

Funding

This work was supported by Wuxi Science and Technology Bureau Science and Technology Research Project (Medical and Health Technology Research) (Y20212043).

Ethics approval

All procedures performed in studies involving human participants were in accordance with the ethical standards of the institutional and/or national research committee and with the Helsinki Declaration and its later amendments or comparable ethical standards. The study was approved by the Ethics Committee of Third Affiliated Hospital of Nanjing University of Traditional Chinese Medicine Hospital (approval no. KY2017004).

Author contributions

Weiqing Qian and Xudong Chu designed experiments. Haitao Sun, Lining Wang Yuanyuan Niu and Tianchi Zhang carried out experiments. Muzhe Li, Bin Xu and Yong Ma analyzed experimental results.

Data availability

The datasets used and/or analyzed during the current study are available from the corresponding author on reasonable request.

Acknowledgement

We thank the Wuxi Science and Technology Bureau Science and Technology Research Project (Medical and Health Technology Research).

Conflict of interest

The authors declare that they have no competing interests.

Consent for publication

Not applicable.

References

1. Shen Y, Gray DL and Martinez DS (2017) Combined Pharmacologic Therapy in Postmenopausal Osteoporosis. Endocrinol Metab Clin North Am 46:193-206. doi: 10.1016/j.ecl.2016.09.008
2. Rizzoli R (2018) Postmenopausal osteoporosis: Assessment and management. Best Pract Res Clin Endocrinol Metab 32:739-757. doi: 10.1016/j.beem.2018.09.005
3. Qiu Y, Yang W, Wang Q, Yan S, Li B and Zhai X (2018) Osteoporosis in postmenopausal women in this decade: a bibliometric assessment of current research and future hotspots. Arch Osteoporos 13:121. doi: 10.1007/s11657-018-0534-5

4. Migliorini F, Colarossi G, Baroncini A, Eschweiler J, Tingart M and Maffulli N (2021) Pharmacological Management of Postmenopausal Osteoporosis: a Level I Evidence Based - Expert Opinion. Expert Rev Clin Pharmacol 14:105-119. doi: 10.1080/17512433.2021.1851192
5. Tsai JN, Lee H, David NL, Eastell R and Leder BZ (2019) Combination denosumab and high dose teriparatide for postmenopausal osteoporosis (DATA-HD): a randomised, controlled phase 4 trial. Lancet Diabetes Endocrinol 7:767-775. doi: 10.1016/S2213-8587(19)30255-4
6. Li H and Li L (2018) [Low magnitude whole-body vibration and postmenopausal osteoporosis]. Sheng Wu Yi Xue Gong Cheng Xue Za Zhi 35:301-306. doi: 10.7507/1001-5515.201801071
7. Soni S, Torvund M and Mandal CC (2021) Molecular insights into the interplay between adiposity, breast cancer and bone metastasis. Clin Exp Metastasis 38:119-138. doi: 10.1007/s10585-021-10076-0
8. Hernigou P (2020) The history of bone marrow in orthopaedic surgery (part I trauma): trepanning, bone marrow injection in damage control resuscitation, and bone marrow aspiration to heal fractures. Int Orthop 44:795-808. doi: 10.1007/s00264-020-04506-z
9. Fischer V and Haffner-Luntzer M (2021) Interaction between bone and immune cells: Implications for postmenopausal osteoporosis. Semin Cell Dev Biol. doi: 10.1016/j.semcdb.2021.05.014
10. Lee JS, Lee JM and Im GI (2011) Electroporation-mediated transfer of Runx2 and Osterix genes to enhance osteogenesis of adipose stem cells. Biomaterials 32:760-8. doi: 10.1016/j.biomaterials.2010.09.042
11. Hutchings G, Moncrieff L, Dompe C, Janowicz K, Sibiak R, Bryja A, Jankowski M, Mozdziak P, Bukowska D, Antosik P, Shibli JA, Dyszkiewicz-Konwinska M, Bruska M, Kempisty B and Piotrowska-Kempisty H (2020) Bone Regeneration, Reconstruction and Use of Osteogenic Cells; from Basic Knowledge, Animal Models to Clinical Trials. J Clin Med 9. doi: 10.3390/jcm9010139
12. D'Angelo E and Agostini M (2018) Long non-coding RNA and extracellular matrix: the hidden players in cancer-stroma cross-talk. Noncoding RNA Res 3:174-177. doi: 10.1016/j.ncrna.2018.08.002
13. Jothimani G, Sriramulu S, Chabria Y, Sun XF, Banerjee A and Pathak S (2018) A Review on Theragnostic Applications of Micrornas and Long Non- Coding RNAs in Colorectal Cancer. Curr Top Med Chem 18:2614-2629. doi: 10.2174/1568026619666181221165344
14. Ji E, Kim C, Kim W and Lee EK (2020) Role of long non-coding RNAs in metabolic control. Biochim Biophys Acta Gene Regul Mech 1863:194348. doi: 10.1016/j.bbagrm.2018.12.006
15. Jin D, Wu X, Yu H, Jiang L, Zhou P, Yao X, Meng J, Wang L, Zhang M and Zhang Y (2018) Systematic analysis of lncRNAs, mRNAs, circRNAs and miRNAs in patients with postmenopausal osteoporosis. Am J Transl Res 10:1498-1510.
16. Zheng D, Wang B, Zhu X, Hu J, Sun J, Xuan J and Ge Z (2019) LncRNA OIP5-AS1 inhibits osteoblast differentiation of valve interstitial cells via miR-137/TWIST11 axis. Biochem Biophys Res Commun 511:826-832. doi: 10.1016/j.bbrc.2019.02.109
17. Carreca AP, Pravata VM, Markham M, Bonelli S, Murphy G, Nagase H, Troeberg L and Scilabra SD (2020) TIMP-3 facilitates binding of target metalloproteinases to the endocytic receptor LRP-1 and

promotes scavenging of MMP-1. Sci Rep 10:12067. doi: 10.1038/s41598-020-69008-9

18. Black DM and Rosen CJ (2016) Clinical Practice. Postmenopausal Osteoporosis. N Engl J Med 374:254-62. doi: 10.1056/NEJMcp1513724
19. Xu H, Liu T, Hu L, Li J, Gan C, Xu J, Chen F, Xiang Z, Wang X and Sheng J (2019) Effect of caffeine on ovariectomy-induced osteoporosis in rats. Biomed Pharmacother 112:108650. doi: 10.1016/j.biopha.2019.108650
20. Wang C, Zhang L, Ndong JC, Hettinghouse A, Sun G, Chen C, Zhang C, Liu R and Liu CJ (2019) Progranulin deficiency exacerbates spinal cord injury by promoting neuroinflammation and cell apoptosis in mice. J Neuroinflammation 16:238. doi: 10.1186/s12974-019-1630-1
21. Couto de Carvalho LA, Tosta Dos Santos SL, Sacramento LV, de Almeida VRJ, de Aquino Xavier FC, Dos Santos JN and Gomes Henriques Leitao AC (2020) Mesenchymal stem cell markers in periodontal tissues and periapical lesions. Acta Histochem 122:151636. doi: 10.1016/j.acthis.2020.151636
22. Wang H, Zhou K, Xiao F, Huang Z, Xu J, Chen G, Liu Y and Gu H (2020) Identification of circRNA-associated ceRNA network in BMSCs of OVX models for postmenopausal osteoporosis. Sci Rep 10:10896. doi: 10.1038/s41598-020-67750-8
23. Lin W, Zhu X, Gao L, Mao M, Gao D and Huang Z (2021) Osteomodulin positively regulates osteogenesis through interaction with BMP2. Cell Death Dis 12:147. doi: 10.1038/s41419-021-03404-5
24. Li W, Zhu HM, Xu HD, Zhang B and Huang SM (2018) CRNDE impacts the proliferation of osteoclast by estrogen deficiency in postmenopausal osteoporosis. Eur Rev Med Pharmacol Sci 22:5815-5821. doi: 10.26355/eurrev_201809_15907
25. Wang Q, Li Y, Zhang Y, Ma L, Lin L, Meng J, Jiang L, Wang L, Zhou P and Zhang Y (2017) LncRNA MEG3 inhibited osteogenic differentiation of bone marrow mesenchymal stem cells from postmenopausal osteoporosis by targeting miR-133a-3p. Biomed Pharmacother 89:1178-1186. doi: 10.1016/j.biopha.2017.02.090
26. Wu ZH, Huang KH, Liu K, Wang GT and Sun Q (2018) DGCR5 induces osteogenic differentiation by up-regulating Runx2 through miR-30d-5p. Biochem Biophys Res Commun 505:426-431. doi: 10.1016/j.bbrc.2018.09.033
27. Wang X, Zhao D, Zhu Y, Dong Y and Liu Y (2019) Long non-coding RNA GAS5 promotes osteogenic differentiation of bone marrow mesenchymal stem cells by regulating the miR-135a-5p/FOXO1 pathway. Mol Cell Endocrinol 496:110534. doi: 10.1016/j.mce.2019.110534
28. Li M, Cong R, Yang L, Yang L, Zhang Y and Fu Q (2020) A novel lncRNA LNC_000052 leads to the dysfunction of osteoporotic BMSCs via the miR-96-5p-PIK3R1 axis. Cell Death Dis 11:795. doi: 10.1038/s41419-020-03006-7
29. Han HS, Ju F and Geng S (2018) In vivo and in vitro effects of PTH1-34 on osteogenic and adipogenic differentiation of human bone marrow-derived mesenchymal stem cells through regulating microRNA-155. J Cell Biochem 119:3220-3235. doi: 10.1002/jcb.26478

30. Zheng HB, Wu M, Zhang G and Chen KL (2021) MicroRNA-182 inhibits osteogenic differentiation of bone marrow mesenchymal stem cells by targeting Smad1. J Biol Regul Homeost Agents 35:505-516. doi: 10.23812/20-688-A
31. Wang F, Tan WH, Liu W, Jin YX, Dong DD, Zhao XJ and Liu Q (2020) Effects of miR-214 on cervical cancer cell proliferation, apoptosis and invasion via modulating PI3K/AKT/mTOR signal pathway. Eur Rev Med Pharmacol Sci 24:7573. doi: 10.26355/eurrev_202007_22242
32. Peng R, Cheng X, Zhang Y, Lu X and Hu Z (2020) miR-214 down-regulates MKK3 and suppresses malignant phenotypes of cervical cancer cells. Gene 724:144146. doi: 10.1016/j.gene.2019.144146
33. Zhang H, Sun P, Wang YL, Yu XF and Tong JJ (2020) MiR-214 promotes proliferation and inhibits apoptosis of oral cancer cells through MAPK/ERK signaling pathway. Eur Rev Med Pharmacol Sci 24:3710-3716. doi: 10.26355/eurrev_202004_20834
34. Yang L, Ge D, Cao X, Ge Y, Chen H, Wang W and Zhang H (2016) MiR-214 Attenuates Osteogenic Differentiation of Mesenchymal Stem Cells via Targeting FGFR1. Cell Physiol Biochem 38:809-20. doi: 10.1159/000443036
35. Li QS, Meng FY, Zhao YH, Jin CL, Tian J and Yi XJ (2017) Inhibition of microRNA-214-5p promotes cell survival and extracellular matrix formation by targeting collagen type IV alpha 1 in osteoblastic MC3T3-E1 cells. Bone Joint Res 6:464-471. doi: 10.1302/2046-3758.68.BJR-2016-0208.R2
36. Salazar VS, Zarkadis N, Huang L, Norris J, Grimston SK, Mbalaviele G and Civitelli R (2013) Embryonic ablation of osteoblast Smad4 interrupts matrix synthesis in response to canonical Wnt signaling and causes an osteogenesis-imperfecta-like phenotype. J Cell Sci 126:4974-84. doi: 10.1242/jcs.131953
37. Kuang W, Zheng L, Xu X, Lin Y, Lin J, Wu J and Tan J (2017) Dysregulation of the miR-146a-Smad4 axis impairs osteogenesis of bone mesenchymal stem cells under inflammation. Bone Res 5:17037. doi: 10.1038/boneres.2017.37
38. Ma X, Fan C, Wang Y, Du Y, Zhu Y, Liu H, Lv L, Liu Y and Zhou Y (2020) MiR-137 knockdown promotes the osteogenic differentiation of human adipose-derived stem cells via the LSD1/BMP2/SMAD4 signaling network. J Cell Physiol 235:909-919. doi: 10.1002/jcp.29006
39. Xie H, Liu M, Jin Y, Lin H, Zhang Y and Zheng S (2020) miR-1323 suppresses bone mesenchymal stromal cell osteogenesis and fracture healing via inhibiting BMP4/SMAD4 signaling. J Orthop Surg Res 15:237. doi: 10.1186/s13018-020-01685-8
40. Xu Y, Jin Y, Hong F, Ma Y, Yang J, Tang Y, Zhu Z, Wu J, Bao Q, Li L, Yao B, Li D and Ma C (2021) MiR-664-3p suppresses osteoblast differentiation and impairs bone formation via targeting Smad4 and Osterix. J Cell Mol Med 25:5025-5037. doi: 10.1111/jcmm.16451

Figures

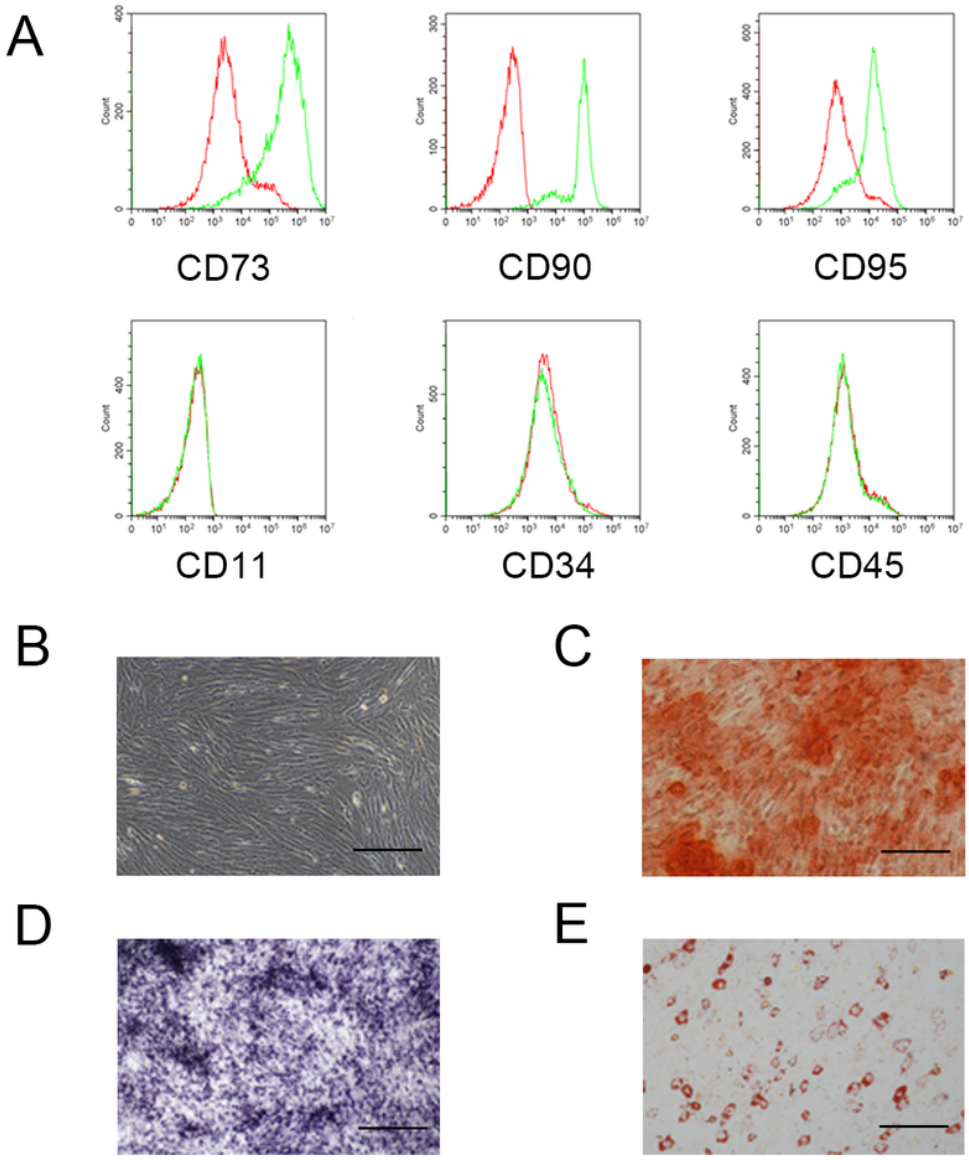

Figure 1

Characteristics of BMSCs. (A) Contents of surface markers including CD73, CD90, CD95, CD11, CD34 and CD45 were detected by flow cytometry assay. (B) Morphology of BMSCs when confluence reached 90%. (C) Alizarin red and (D) ALP staining images of BMSCs after osteogenic induction. (E) Oil Red O staining image of BMSCs after adipogenic induction. Scale bar: 200μm. BMCSs, bone marrow mesenchymal stem cells; ALP, alkaline phosphatase.

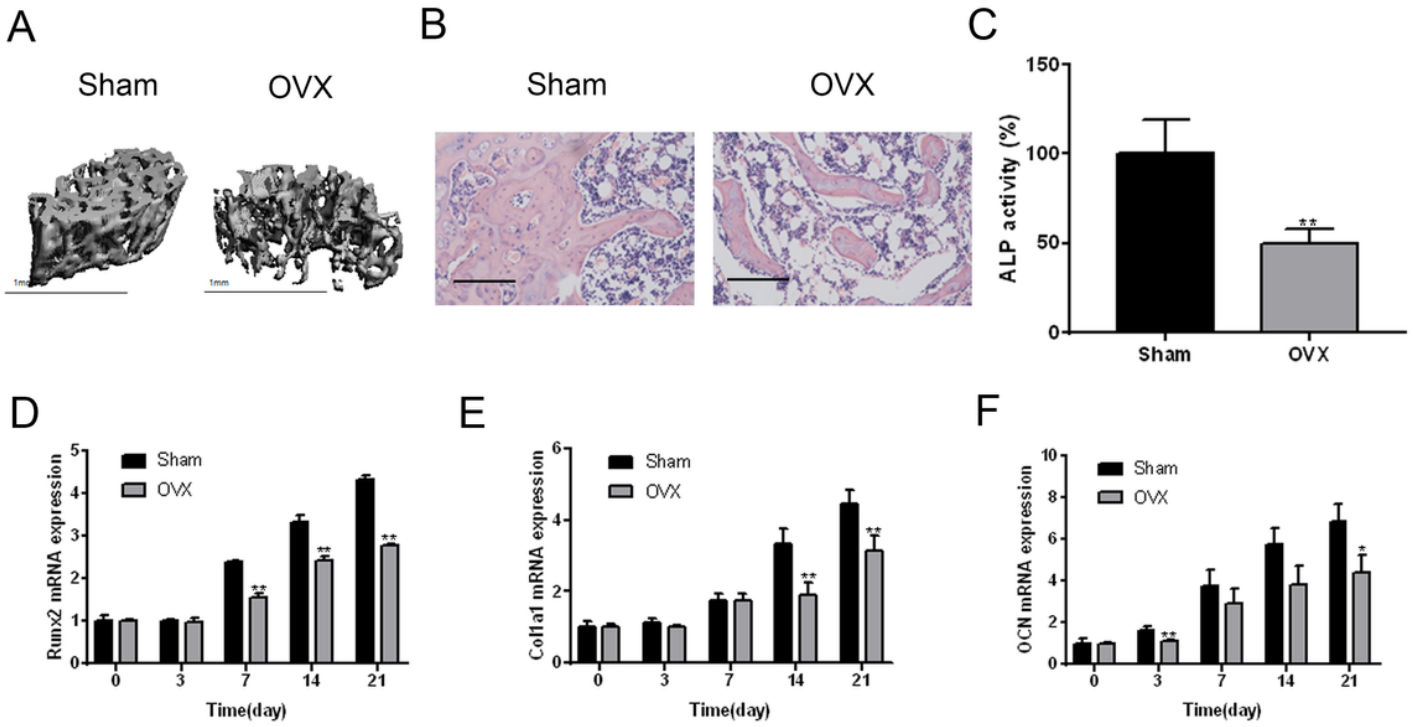

Figure 2

Osteogenic capability was notably weakened in OVX rats. (A) Micro-CT image of vertebral trabecula isolated from PMOP rat model. (B) HE staining image of vertebral paraffin section. (C) ALP activity in the L4 vertebra of PMOP rat model. (D-F) mRNA expression levels of Runx2, Col1a1 and OCN in PMOP rat model were detected 0, 3, 7, 14 and 21 days after modeling. Scale bar: 200μm. Each assay was performed for triplication. $^{**}P < 0.01$ vs. sham; $^{*}P < 0.05$ vs. sham. OVX, ovariectomy; PMOP, postmenopausal osteoporosis; ALP, alkaline phosphatase; OCN, osteocalcin.

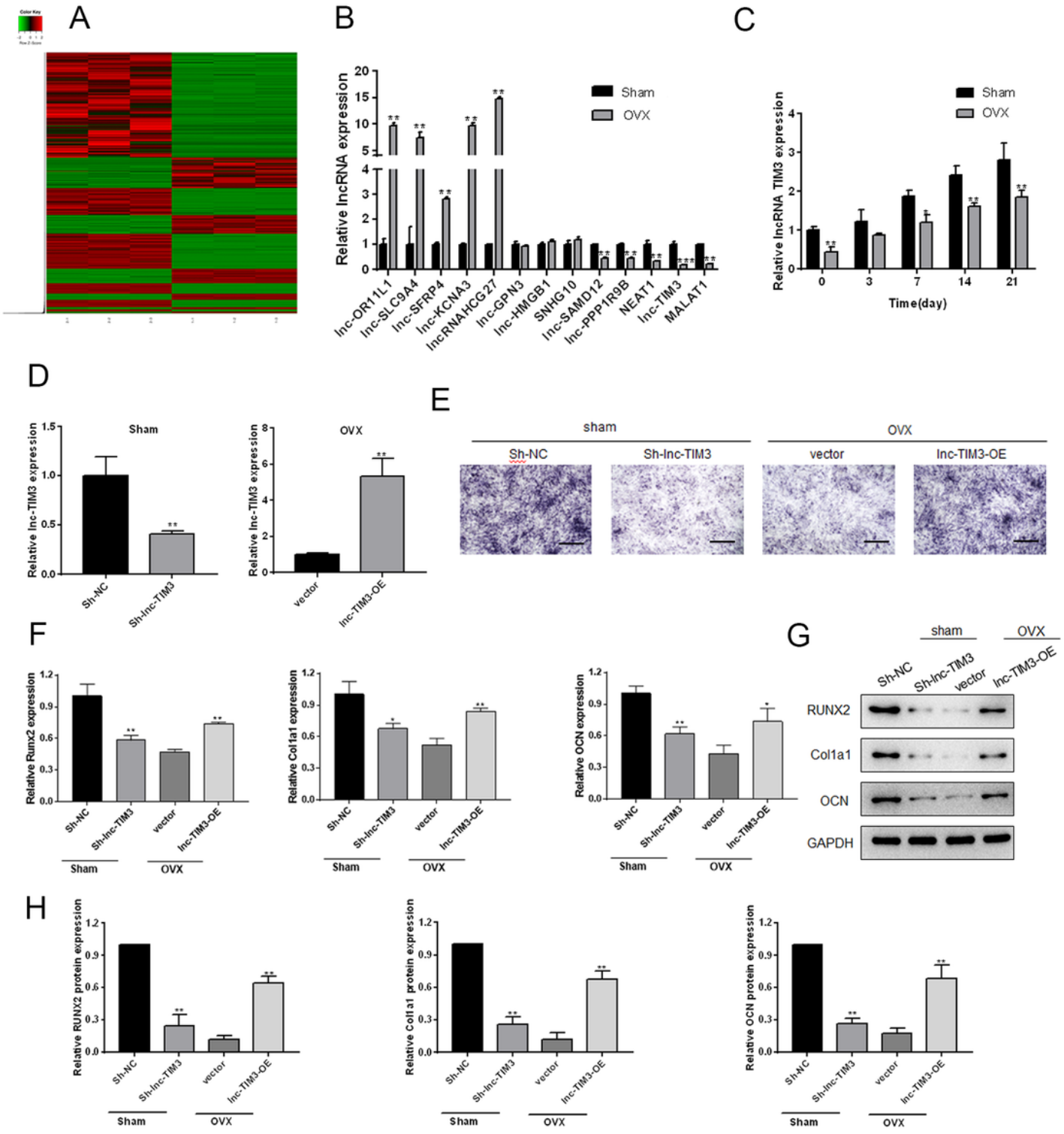

Figure 3

lncTIM3 was downregulated in PMOP and promoted osteogenic differentiation of BMSCs. (A) RNA sequencing of the PMOP DE lncRNAs in clinical samples. (B) RT-qPCR was used to verify the sequencing results. (C) lncTIM3 expression levels in PMOP rat model 0, 3, 7, 14 and 21 days after modeling. (D) lncTIM3 expression levels when BMSCs transfected with sh-lncTIM3 or pcDNA3.1/lncTIM3. (E) ALP-positive BMSCs under the indicated treatments. (F) mRNA and (G and H) protein expression levels of

Runx2, Col1a1 and OCN under the indicated treatments. Scale bar: 200μm. Each assay was performed for triplication. **P < 0.01 vs. sh-NC or vector; *P < 0.05 vs. sh-NC or vector. BMCSs, bone marrow mesenchymal stem cells; PMOP, postmenopausal osteoporosis; ALP, alkaline phosphatase; OCN, osteocalcin.

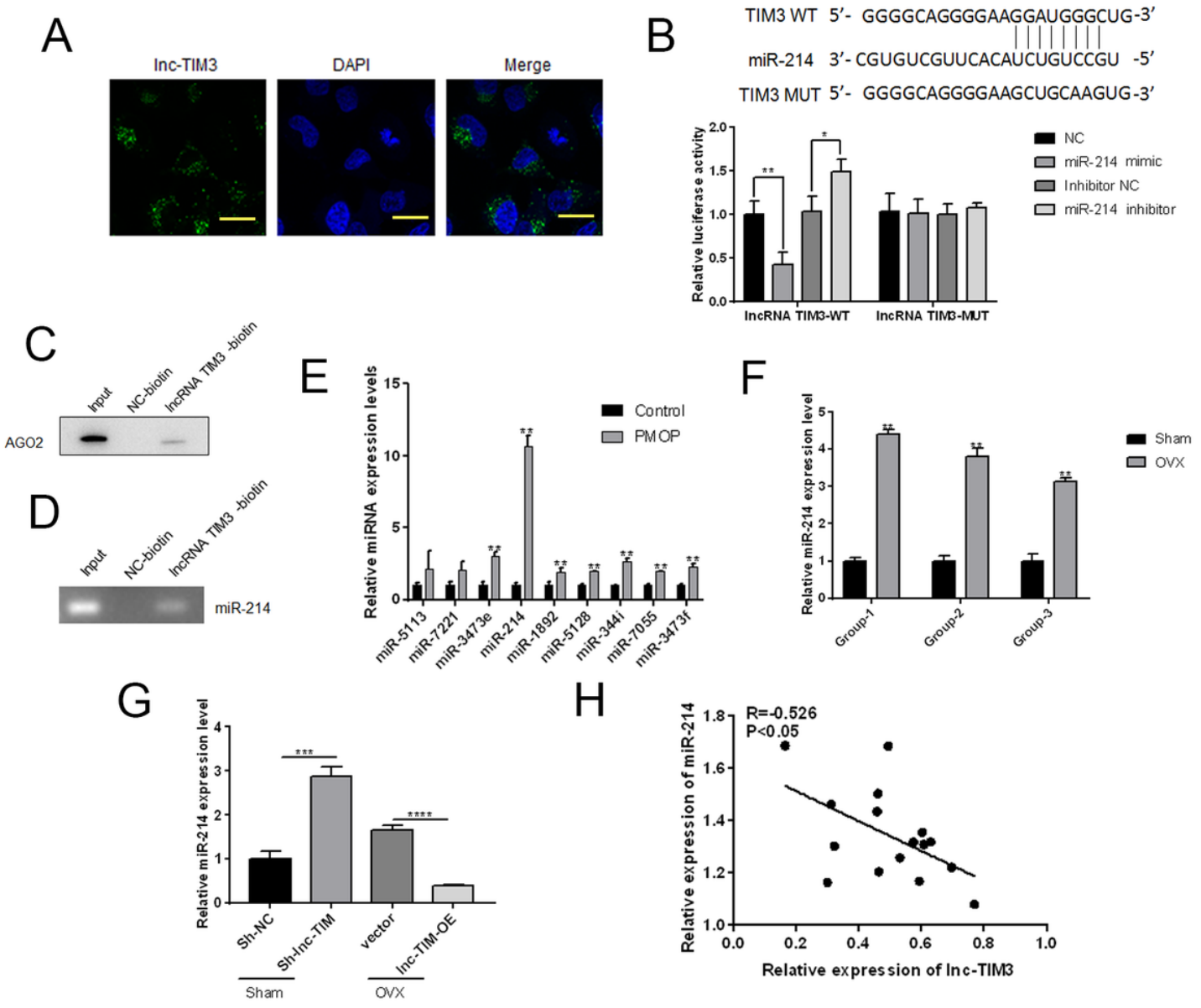

Figure 4

lncTIM3 sponged for miR-214 in BMSCs. (A) FISH images of lncTIM3 in BMSCs. (B) Luciferase reporter assay was conducted to verify the targeting relationship between lncTIM3 and miR-214. RNA pull-down assay for (C) Ago2 and (D) miR-214 using biotinylated lncTIM3. (E) Detection of the osteogenesis-related miRNAs in the clinical samples. (F) Expression levels of miR-214 in 3 groups of PMOP rat models. (G) Expression levels of miR-214 in BMSCs transfected with sh-lncTIM3 or pcDNA3.1/lncTIM3. (H) Pearson correlation analysis between the expression levels of miR-214 and lncTIM3 in PMOP. Scale bar: 200μm. Each assay was performed for triplication. **P < 0.01 vs. OVX, sh-NC or vector; *P < 0.05. FISH,

fluorescence in situ hybridization; BMCSs, bone marrow mesenchymal stem cells; PMOP, postmenopausal osteoporosis.

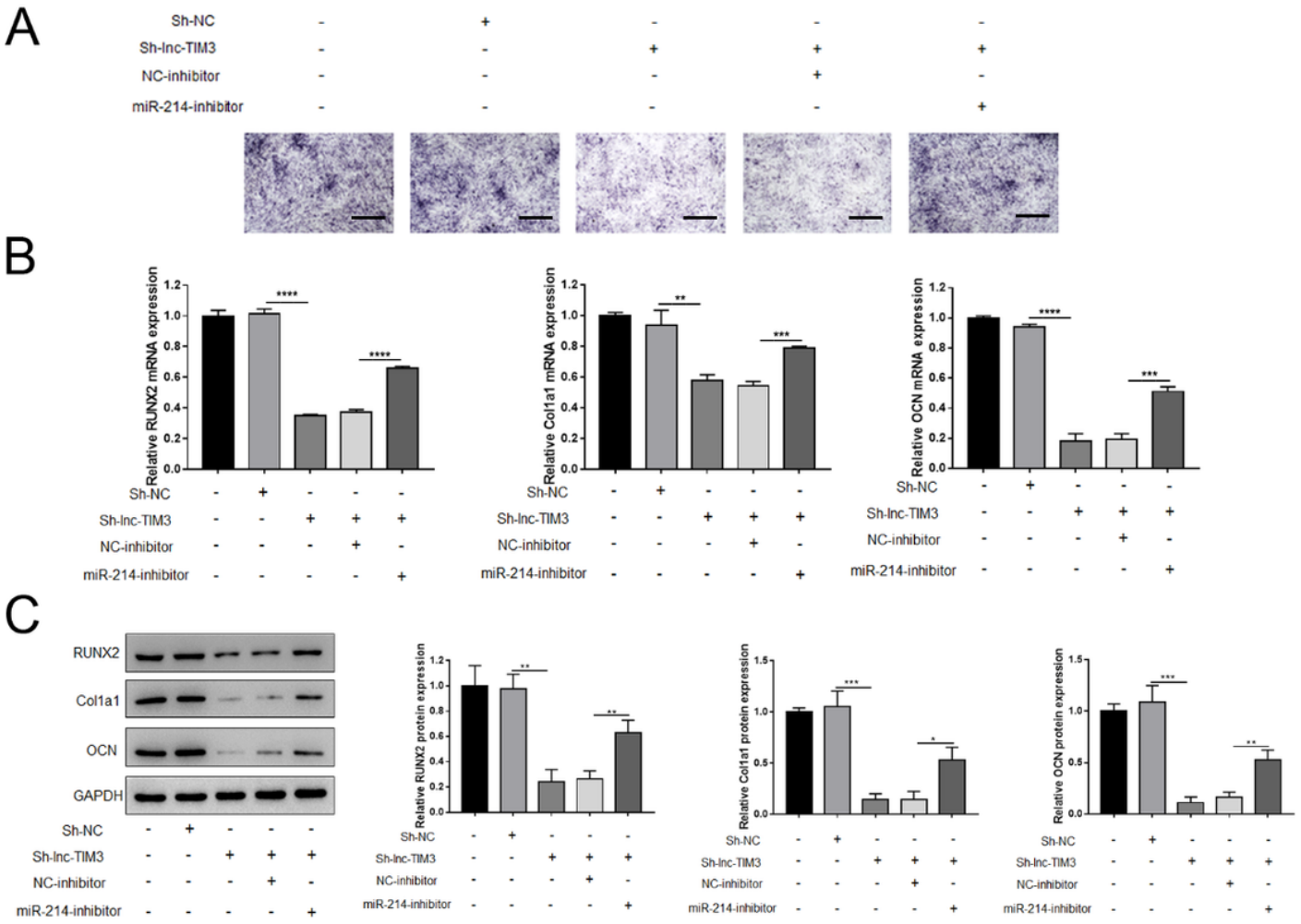

Figure 5

miR-214 inhibitor abrogated the effects of sh-lncTIM3 on osteogenic induction. (A) ALP staining images of BMSCs transfected with miR-214 inhibitor and sh-lncTIM3. (B) mRNA and (C) protein expression levels of Runx2, Col1a1 and OCN in BMSCs transfected with miR-214 inhibitor and sh-lncTIM3. Scale bar: 200μm. Each assay was performed for triplication. $^{****}P < 0.0001$; $^{***}P < 0.001$; $^{**}P < 0.01$; $^{*}P < 0.05$. BMCSs, bone marrow mesenchymal stem cells; ALP, alkaline phosphatase; OCN, osteocalcin.

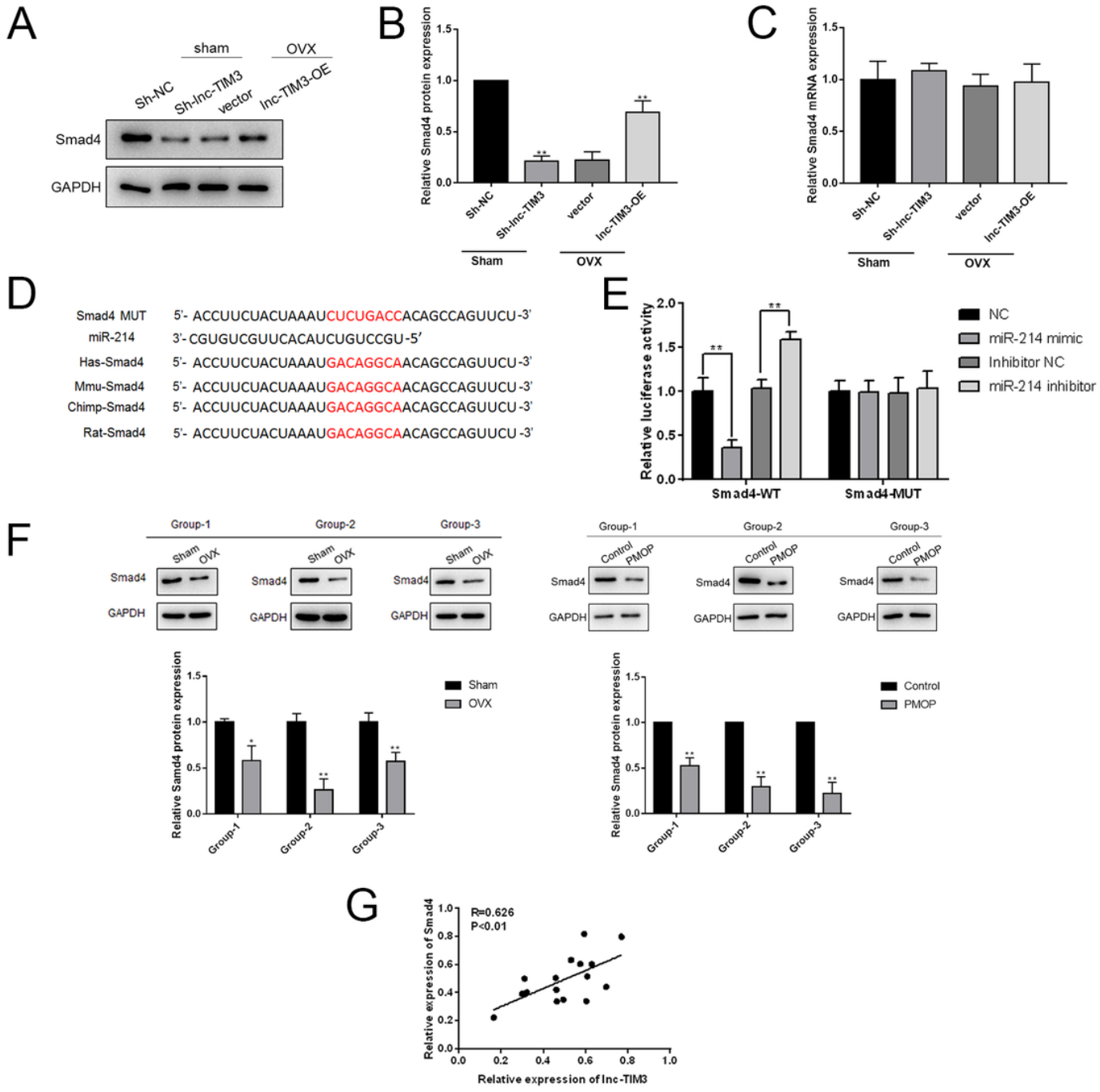

Figure 6

Smad4 was the target gene of miR-214. (A) The gel electrophoresis images of Smad4 that were extracted from the BMSCs of the rat model. (B) Quantification of (A). (C) mRNA expression levels of Smad4 after sh-lncTIM3 or lncTIM3 OE treatment. (D) Sequences of 3'-UTR of Smad4 WT, MUT and miR-214. (E) Luciferase activities of WT and MUT Smad4 treated with miR-214 mimic or inhibitor. (F) Protein expressions of Smad4 in 3 groups of OVX rat models and PMOP clinical samples. (G) Pearson correlation analysis between expressions of miR-214 and Smad4. Each assay was performed for triplication. $^{**}P < 0.01$; $^{*}P < 0.05$. BMCSs, bone marrow mesenchymal stem cells; ALP, alkaline phosphatase; OCN, osteocalcin.

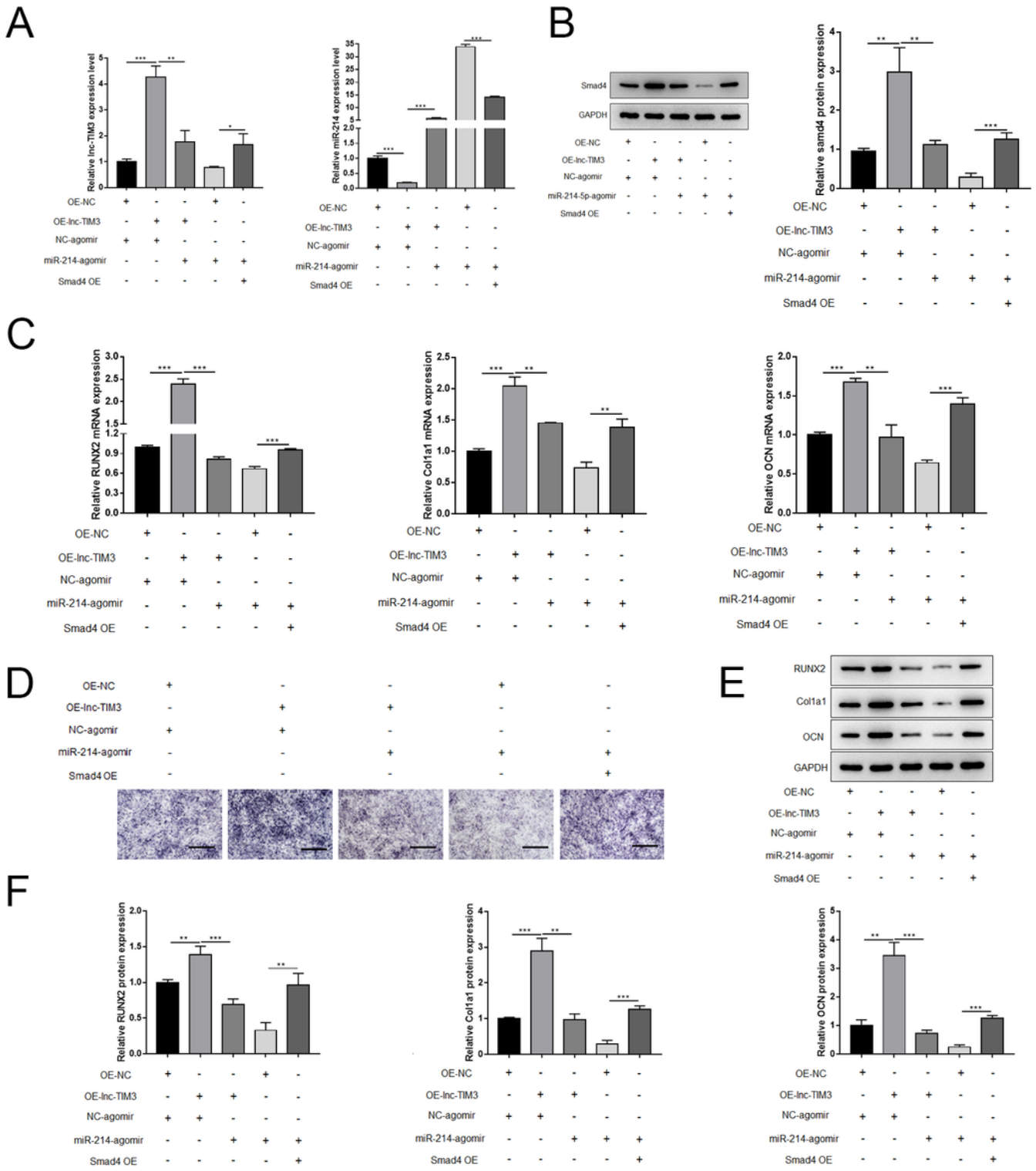

Figure 7

Smad4 was the target gene of miR-214. (A) The gel electrophoresis images of Smad4 that were extracted from the BMSCs of the rat model. (B) Quantification of (A). (C) mRNA expression levels of Smad4 after sh-lncTIM3 or lncTIM3 OE treatment. (D) Sequences of 3'-UTR of Smad4 WT, MUT and miR-214. (E) Luciferase activities of WT and MUT Smad4 treated with miR-214 mimic or inhibitor. (F) Protein expressions of Smad4 in 3 groups of OVX rat models and PMOP clinical samples. (G) Pearson

correlation analysis between expressions of miR-214 and Smad4. Each assay was performed for triplication. $^{**}P < 0.01$; $^{*}P < 0.05$. BMCSs, bone marrow mesenchymal stem cells; ALP, alkaline phosphatase; OCN, osteocalcin.